phase. The nature of this observation will be discussed briefly later.

Thus, the qualitative model that emerges for this new phase is one in which the elongated molecules are arranged in loosely ordered layers with their long axes either normal to or only slightly tilted with respect to the layer planes. In the direction of the layer planes there is a twist in the parallel orientation of the molecules. This twist can be effected either by defects, such as screw dislocations, between short sections of the A phase, or by cholesteric liquid-like regions separating larger smectic-A domains, as shown in Fig. 1. The full structural details of this phase are now being studied by high-resolution X-ray diffraction from aligned samples and by freeze-fracture studies. The results obtained from these investigations will be reported soon.

Finally, we note that de Gennes[13] has predicted that, just as magnetic flux can penetrate Type II superconductors in a lattice of vortices, twist or bend distortions can be incorporated into a layered A structure by the presence of an array of screw or edge dislocations. A model for such an array was proposed recently by Renn and Lubensky[14]. With reference to the structure of the A* phase shown in Fig. 1, their model specifies that grain boundaries of screw dislocations are responsible for rotating the individual 'blocks' of the A* layers with respect to each other. They call the resultant phase a twist-grain-boundary (TGB) phase, and predict that it can occur between the cholesteric and the A phase in a manner similar to the occurrence of the Abrikosov flux-lattice phase between normal and superconducting phases[15]. Renn and Lubensky established that the requirement for this intermediate phase to occur is that the Ginzburg parameter, which is equal to the ratio of the twist penetration length (λ_T) to the smectic-A correlation length (ξ), must be greater than $1/\sqrt{2}$.

Consequently, the TGB phase is a feasible model for the A* phase, for the following reasons. First, the X-ray scattering pattern predicted for the TGB phase is consistent with our X-ray measurements on the A* phase. Second, the model predicts a helical structure with the helical axis parallel to the smectic layers, which is consistent with our optical experiments. Finally, we observe the A* phase in the vicinity of an A→C* transition, where the A phase is stable over a short temperature range. At such a transition, λ_T diverges, resulting in a large value for the Ginzberg parameter, as required by the theory (R. B. Meyer, personal communication). Assuming that the TGB phase is a viable model for the A* phase, we can explore the possible implications of this phenomenon still further. In particular, we can speculate on the nature of the effect observed near to the clearing point in the isotropic liquid. For the superconducting flux lattice it has been proposed[16] and observed[17] that the vortex lattice can disorder into an entangled or disentangled fluid of vortices. We suggest that a similar disordering of the regular array of screw dislocations in the TGB phase may be the mechanism responsible for the occurrence of the effect observed in the isotropic liquid at a temperature just above the transition from the A* phase.

Received 23 August; accepted 9 December 1988.

1. Reinitzer, F. *Monatsh. Chemie* **9**, 421-425 (1888).
2. Lehmann, O. *Z. phys. Chem. (Leipzig)* **4**, 462-468 (1889).
3. Chin, E. & Goodby, J. W. *Mol. Cryst. Liq. Cryst.* **141**, 311-320 (1986).
4. Meyer, R. B. *Mol. Cryst. Liq. Cryst.* **40**, 33-48 (1977).
5. Goodby, J. W. & Chin, E. *Liq. Cryst.* **3**, 1245-1254 (1988).
6. Grandjean, F. *Compt. Rend.* **172**, 71-74 (1921); **166**, 165-167 (1917).
7. Glogarova, M., Lejek, L., Pavel, J., Janovec, U. & Fousek, F. *Mol. Cryst. Liq. Cryst.* **91**, 309-325 (1983).
8. Patel, J. S., Leslie, T. M. & Goodby, J. W. *Ferroelectrics* **59**, 137-144 (1984).
9. Patel, J. S. & Goodby, J. W. *J. appl. Phys.* **59**, 2355-2360 (1986).
10. Friedel, G. *Ann. Phys. (Paris)* **18**, 273-473 (1922).
11. Goodby, J. W., Chin, E., Leslie, T. M., Geary, J. M. & Patel, J. S. *J. Am. chem. Soc.* **108**, 4729-4735 (1986).
12. Sackmann, H. & Demus, D. *Mol. Cryst. Liq. Cryst.* **2**, 81-102 (1966).
13. De Gennes, P. G. *Solid St. Commun.* **10**, 753-756 (1972).
14. Renn, S. R. & Lubensky, T. C. *Phys. Rev.* A (submitted).
15. Abrikosov, A. A. *Sov. Phys. JETP* **5**, 1174-1178 (1957).
16. Nelson, D. R. *Phys. Rev. Lett.* **60**, 1973-1976 (1988).
17. Gammel, P. L. *et al. Phys. Rev. Lett.* **59**, 2592-2595 (1987).

Disequilibrium of Holocene sediment yield in glaciated British Columbia

Michael Church & Olav Slaymaker

Department of Geography, University of British Columbia, Vancouver, British Columbia, Canada V6T 1W5

It is generally supposed that specific sediment yield—the quantity of sediment passing a monitored river cross-section per unit area drained upstream of that section—declines as the area drained increases[1-3]. Part of the sediment mobilized from the land surface is supposed to go back into storage at field edges, and on footslopes and floodplains. In contrast, we show here that data from British Columbian rivers reveal a pattern of increasing specific sediment yield at all spatial scales up to 3×10^4 km^2. This results from the dominance of secondary remobilization of Quaternary sediments along river valleys over primary denudation of the land surface. The result controverts the conventional model which has been derived from studies of small, highly disturbed agricultural catchments. The rivers are still responding to the last glaciation, giving a landscape relaxation time greater than 10 kyr. This holds profound implications for geomorphological theory and for studies of erosion.

Happ and others[4-6] have shown that specific sediment yield presently increases downstream in the south-eastern United States, which they explained in terms of remobilization of sediment eroded from uplands during the first two centuries of European agrarian settlement. Schumm[7] has asserted that such a complex response to episodes of upland erosion is the usual pattern of river-basin development, but apart from a speculation by Meade[8] that the response in this region may persist for centuries, little has been said about the timescales of adjustment of the fluvial landscape to perturbations in sediment supply, nor has the conventional model been tested critically in natural landscapes.

Our main data resource is the archive of suspended sediment loads obtained by the Water Survey of Canada since 1965. These data (Fig. 1) have been discussed at length elsewhere[9,10]. Here we emphasize only that they represent contemporary fluvial sediment transfers in British Columbian rivers. Bedload transport, which is not normally measured, accounts for a comparatively small proportion of the total load[11]. Although solutes may be significant, they do not alter the pattern presented in Fig. 1[9]. The data have been augmented by results from research studies of small drainage basins[9,12], which allow us to extend the domain of drainage areas by two orders of magnitude. We have classified basins according to whether (1) they contain contemporary glaciers, (2) they contain large lakes or reservoirs, (3) they have been disturbed by human land use, including mining and contemporaneous clearance of more than 5 per cent of the forest, and (4) they are undisturbed. No basin has a significant proportion ($>5\%$) of arable land.

The relation of sediment yield to drainage area (Fig. 1) is complex, but a clear trend emerges for basins that are classified as undisturbed. Only three such basins plot outside this trend. Specific sediment yield increases through all areas up to about 3×10^4 km^2. Between 40 km^2 and 10^4 km^2, specific yield is approximately proportional to (area)$^{0.6}$, implying a near-linear increase in sediment yield downstream. The local range of the main trend is between about one-half and one order of magnitude in yield: detailed examination of the data[10] indicates that variable Quaternary and bedrock geology is the cause. There is no systematic association, however, between rock type and topography to explain the overall trend, which is replicated within individual major drainage basins.

On the evidence of Fig. 1, primary denudation, indicated by sediment yield in the smallest basins, is more than an order of

Table 1 Comparison of predicted and measured streambank erosion

River	h (m)	M (m yr^{-1})	dY/dL* (Mg m^{-1} yr^{-1})	A_d (km^2)	Predicted range of dY/dL†	Comments
Liard and Peace River systems‡						
Sikanni Chief	8.3	2.9	13.8	10,530	7.0–38	Sand bed
Fontas	6.5	2.9	9.9	8,110	5.4–30	Sand bed. M assumed
Muskwa	4.0	2.7	4.0	1,510	0.8–4.1	Gravel bed
Prophet	6.0	2.3	7.0	6,765	5.3–29	Gravel bed
Fort Nelson	7.0	4.4	16.5	47,815	32–173	Sand bed. A_d > limit
			(From actual envelopes in Fig. 1:		16–87)	of increasing yields
Beatton	7.0	0.5	1.9	4,070	1.8–10	Fine gravel. M from Nanson[21]
Upper Fraser River system						
Upper Eagle	3.5	1.3	1.5	150	0.10–0.6	Gravel bed. Disturbed?
Lower Eagle	5.0	0.7	1.6	1,385	0.6–3.3	Sand bed

h = mean bank height; M = mean meander migration rate on bend axis. Data from refs 14, 15.
* Calculated as $1.5\,(h-2)M/2$; 1.5 (Mg m^{-3}) is the assumed bulk density of bank material, $h-2$ adjusts for bed material in the lower bank, and $M/2$ gives the average erosion rate assuming linear variation around the bend.
† From equations in the text; equation for mainstream length is $L = 1.2\,A_d^{0.6}$
‡ Some of these rivers are identical with ones in our study, but the places of measurement are different.

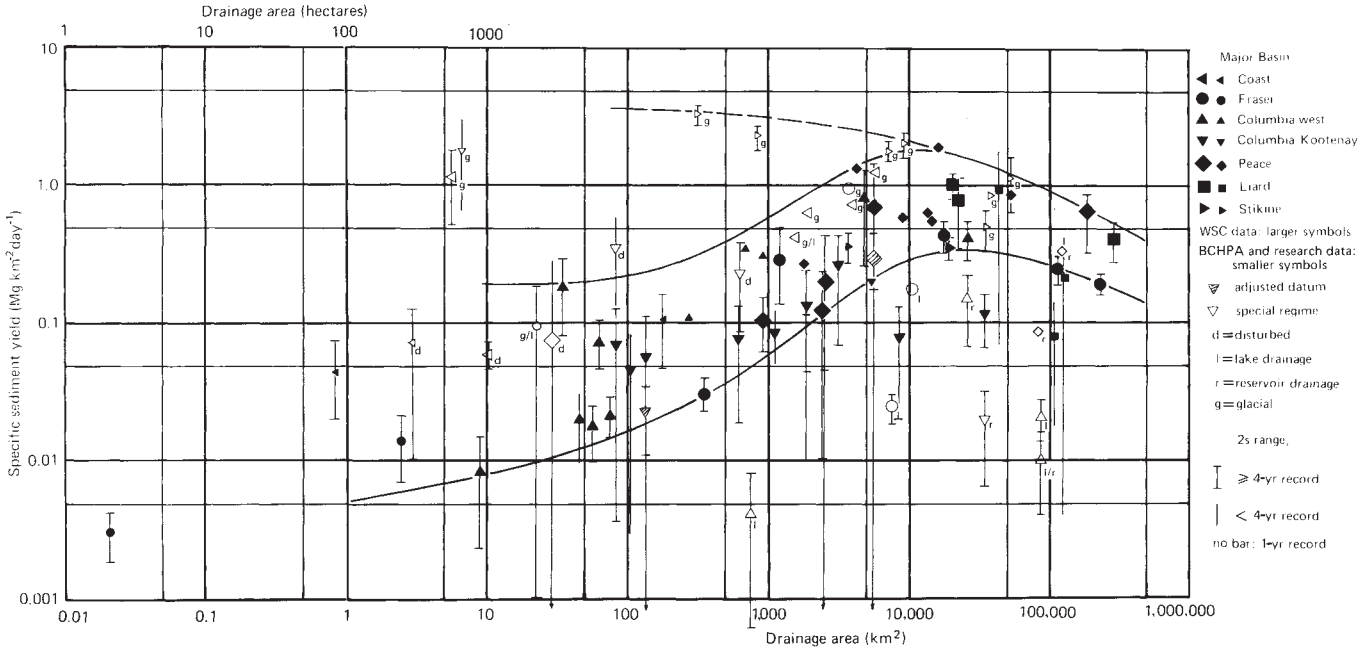

Fig. 1 Specific sediment yield as a function of drainage area for fluvial suspended-sediment-transport records in British Columbian rivers. Closed symbols indicate data for the natural landscape; open symbols indicate yields influenced by natural or human disturbance factors. The main trend of undisturbed yields was sketched by eye. See ref. 10 for a detailed discussion of the data.

magnitude smaller than yield rates in medium to large basins. The latter include a large component arising from secondary remobilization of recent sediments[13]. One must conclude that most of the sediment transported in British Columbian rivers is recruited from the riverbanks and immediate valley-sides. Much of it is derived from the erosion of Quaternary sediments in the valleys and from landsliding of incompetent valley walls.

Thus, the rivers are degrading through valley fill deposits. This is qualitatively evident by the widespread occurrence of Holocene terraces and entrenched trunk streams. We are able to make a quantitative test of our conclusion using data on rates of meander migration obtained by Hickin and Nanson[14,15]. Assuming a linear relation between specific sediment yield and mainstream length (L) for the rising limb of our trend, total sediment yield Y is proportional to A_dL, where A_d is drainage area, so that $dY/dL \propto A_d$. The upper and lower envelopes of our plot are then given approximately by $dY/dL = 36\times10^{-4}\,A_d$ and $dY/dL = 6.5\times10^{-4}\,A_d$, with the coefficients appropriate for units of Mg m^{-1} yr^{-1}. dY/dL is the rate of increase in net erosion downstream, or the net rate of bank erosion if the sediment comes from the stream banks. Table 1 shows that the measurements of Hickin and Nanson generally fall within the range predicted by our analysis. All the results demonstrate that riverbank erosion rates are sufficient to support our interpretation of the regional trend of increasing sediment yield.

The conventional model, in which specific sediment yield decreases with basin area, was derived mainly with reference to intensely cultivated regions in which the land surface is highly disturbed and exposed to erosion[1,2], so that headwater sediment supply is comparatively unlimited. The sediment yield pattern observed in the natural landscape of British Columbia is more consistent with common notions of pristine headwater streams—particularly in mountains—and sediment-laden trunk rivers. A pattern of sediment yield similar to that observed here has been

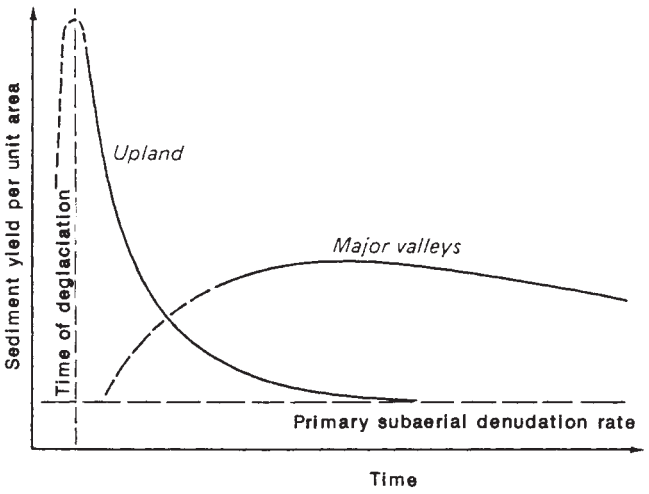

Fig. 2 The paraglacial sedimentation cycle[17], modified to indicate the effect of spatial scale upon the temporal pattern of sediment yield. The time axis spans approximately 10,000 yr.

reported on the Canadian prairies[16], with similar rationalization.

The major rivers are still redistributing sediment that was delivered to the valleys by glacial events more than 10 kyr ago. The transfer and disposition of this material has been termed a 'paraglacial cycle' of sedimentation[17]. Originally, evidence of a paraglacial cycle was adduced from outwash deposits and alluvial fans present in the major valleys, and a relaxation time of a few thousand years was inferred from chronostratigraphic markers in the fans. It is now apparent that this timescale is relevant only for the restricted spatial scale of the upland basins that deliver sediment to the fans. An extended paraglacial cycle (Fig. 2) may be said to dominate still in the larger basins. The trend of specific sediment yield in the largest basins ($>3\times 10^4$ km^2) is consistent with that of contemporary glacierized basins—the most disturbed basins in the region—and conforms approximately with the conventional model. The largest basins are still responding to glaciation. The timescale for ultimate dissipation of this phenomenon appears to be many tens of thousands of years.

It has been supposed for more than 30 years that landscapes adapt so as to reach equilibrium, in some sense, with the imposed environment[18,19], which, for stream systems, implies the hydroclimate[3]. Sediment yield is thereby supposed to be the consequence of erosion from the surface of the land and is supposed to reflect the denudation rate for the prevailing climate and regional geology. This view has been challenged[20] on the basis of observations in the south-eastern United States[4,5]; it certainly is not true at any resolved scale in British Columbia. Fluvial sediment yield at all scales above 1 km^2 remains a consequence of the extraordinary glacial events of the Quaternary Period, rather than of Holocene erosion of the land surface. The results presented here confirm Schumm's contention[7] that fluvial sedimentation does not reflect contemporary erosion of the land surface at any timescale below that for significant evolution of the entire land mass, which is of the order of several ten thousands of years. The natural landscape of British Columbia is imprisoned in its history.

Received 23 August; accepted 7 December 1988.

1. Am. Soc. civil Engng *Sedimentation Engineering* Manuals and Reps on Engng Practice **54**, 458 (1975).
2. Walling, D. E. *J. Hydrology* **65**, 209–237 (1983).
3. Chorley, R. J., Schumm, S. A. & Sugden, D. E. *Geomorphology* 53 and 326 (Methuen, London, 1984).
4. Happ, S. C., Rittenhouse, G. & Dobson, G. C. *U.S. Dept agric. Tech. Bull.* **695** (1940).
5. Meade, R. H. & Trimble, S. W. *Int. Ass. Sci. Hydrol. Publs* **113**, 99–104 (1974).
6. Costa, J. E. *Bull. geol. Soc. Am.* **86**, 1281–1286 (1975).
7. Schumm, S. A. *The Fluvial System* (Wiley, New York, 1978).
8. Meade, R. H. *J. Geol.* **90**, 235–252 (1982).
9. Slaymaker, O. in *International Geomorphology 1986 Part I* (ed. Gardiner, V.) 925–945 (Wiley, Chichester, 1987).
10. Church, M., Kellerhals, R. & Day, T. J. *Can. J. Earth Sci.* (in the press).
11. McLean, D. G. & Church, M. *A reanalysis of sediment transport observations in lower Fraser River* Environment Canada, Inland Waters Dir., Rep. IWD-HQ-WRB-SS-86-2 (1986).
12. Weirich, F. H. *Geografiska Ann.* **67A**, 83–99 (1985).
13. Slaymaker, O. *Int. Ass. Sci. Hydrol. Publs* **122**, 109–117 (1977).
14. Hickin, E. J. & Nanson, G. C. 1984. *J. hydraulic Engng* **110**, 1557–1567 (1984).
15. Nanson, G. C. & Hickin, E. J. *Bull. geol. Soc. Am.* **97**, 497–504 (1986).
16. Ashmore, P. E. *Suspended sediment transport in the Saskatchewan River basin* Environment Canada, Inland Waters Dir., Rep. IWD-HQ-WRB-SS-86-9 (1986).
17. Church, M. & Ryder, J. M. *Bull. geol. Soc. Am.* **83**, 3059–3072 (1972).
18. Strahler, A. H. *Am. J. Sci.* **248**, 673–696 (1950).
19. Hack, J. T. *Am. J. Sci.* **258A**, 80–97 (1960).
20. Trimble, S. W. *Science* **188**, 1207–1208 (1975).
21. Nanson, G. C. thesis, Simon Fraser Univ., Vancouver (1977).

Circadian rhythm and light regulate opsin mRNA in rod photoreceptors

Juan I. Korenbrot* & Russell D. Fernald†

*Departments of Physiology and Biochemistry, School of Medicine, University of California, San Francisco, California 94143 USA
† Institute of Neuroscience, University of Oregon, Eugene, Oregon 97403, USA

Disk membranes in the outer segment of rod photoreceptors are continuously renewed, being assembled at the outer segment base, displaced outward by new disks and eventually shed at the tip[1]. In lower vertebrates, disk assembly occurs with a diurnal rhythm with 2–4% of the outer segment length produced daily[2,3]. We have discovered that in toad and fish retinas the level of mRNA for opsin, the most abundant protein in rod disks[4], fluctuates with a daily rhythm and is regulated both by light and by a circadian oscillator[5]. The mRNA level rises before light onset, remains high during the light phase of a diurnal cycle and decreases four to tenfold during the dark phase. In constant darkness, mRNA elevation occurs during subjective daytime. At night, rod opsin mRNA can be elevated by exposure to light.

The level of rod opsin mRNA was measured by hybridization of an opsin antisense RNA probe to blots of total RNA isolated from the retinas of toads (*Bufo marinus*) and fish (*Haplochromis burtoni*). The opsin RNA probe was synthesized *in vitro* using a fragment subcloned from the bovine rod opsin cDNA (Fig. 1). This fragment is highly conserved in both human[6] and *Drosophila melanogaster*[7] rod opsin, but badly conserved in the rod opsin homologous proteins: β-adrenergic receptor[8] and muscarinic acetylcholine receptor[9]. The use of rod opsin probes across species is also justified by the homology between the visual pigment genes in species ranging from archibacteria to mammals[10].

The specificity of our antisense opsin RNA probe, FH97, in toad and fish tissue was verified by hybridization both to blots of total retinal RNA and *in situ*, to retinal sections. At high stringency hybridization (10–12 °C below the calculated transition temperature for the hybrid assuming perfect nucleotide matching[11]) a single band was detected in autoradiograms of both toad and fish RNA blots (Fig. 1*a*). In toad RNA blots, a fainter, smaller band was occasionally detected. The labelled RNA was 2.85 kilobase (kb) in the toad and 1.4 kb in the fish, suggesting that in toads, but not fish, the rod opsin mRNA includes an untranslated sequence. *In situ* hybridization at identical stringency revealed that the reactive RNA was located exclusively over the myoid region of the photoreceptor inner segments (Fig. 1*b*, *c*).

To determine whether both rod and cone-opsin species were detected by FH97, we used *in situ* hybridization of dark adapted fish retina in which the cone inner segments are displaced relative